

Induction of Indoleamine-2,3-dioxygenase (IDO) in Porcine Aortic Endothelial Cells

J. Aitken,¹ C.T. Dillon,^{1,2} P.A. Lay,¹ R. Stocker,^{3,4} P.K. Witting,^{3,5} Z. Cai,⁶ B. Lai⁶

¹Centre for Heavy Metals Research and Centre for Structural Biology and Structural Chemistry, School of Chemistry, University of Sydney, NSW, Australia

²Current Address: Electron Microscope Unit and the School of Chemistry, University of Sydney, NSW, Australia

³The Heart Research Institute, 145 Missenden Road, Camperdown, Sydney, NSW, Australia

⁴Current Address: Vascular Redox Processes Group, Centre for Vascular Research, School of Medical Sciences, University of New South Wales, UNSW Sydney NSW, Australia

⁵Current Address: Vascular Biology Group, Anzac Research Institute, Hospital Road, Concord Repatriation General Hospital, Concord NSW, Australia

⁶Experimental Facilities Division, Argonne National Laboratory, Argonne, IL, U.S.A.

Introduction

Indoleamine-2,3-dioxygenase (IDO) is a monomeric, glycoprotein (40-45 kDa) containing protoporphyrin IX at the active site [1-3]. In its native ferric form IDO is inactive and requires reductive activation [4, 5]. Once in its active ferrous form, IDO has a high affinity for its main substrate, tryptophan (Trp). Both the Fe(III) and Fe(II) forms of IDO have been studied *in vivo* and *in vitro*. Spectroscopic evidence to date has shown that IDO is similar to typical monomeric heme proteins such as myoglobin (Mb) and leghemoglobin (Lb) [6-9]. As such, IDO is expected to exhibit properties in common with other heme proteins having similar coordination environments. IDO displays ligand binding properties, and a pH dependence, analogous to those of Mb [1, 3].

IDO is found in almost all tissues [2]. Rabbits have the highest levels of IDO in their small intestine, lung and colon, while in mice it is located mainly in the epididymus, colon and small intestine [1]. In humans, it is mostly in the lung, small intestine and placenta [1]. The enzyme can be induced and activated in human monocyte/macrophage cells, murine cells, mononuclear phagocytes and neoplastic cell lines [10].

Many of the activities of interferons (IFN) (the most potent being IFN γ in humans), such as antimicrobial and antiproliferative activity are associated with the induction of IDO and the subsequent depletion of Trp [2, 10, 11, 12]. Interferons are the principal inducers of IDO, both *in vitro* and *in vivo* [2, 11, 12].

While NO is a potentially toxic-free radical, it is also an important signal and effector molecule in the body and as such is involved in the immune, nervous and vascular systems of mammals. It is generated by the breakdown of L-arginine (Arg), which is catalyzed by nitric oxide synthase (NOS) [12]. Nitric oxide reacts rapidly with heme proteins, and it either performs functions in this way or inhibits enzyme activity [12,

13-15]. Recently, it has been found that there is a similarity, and possibly a relationship, between the L-Arg and L-Trp metabolic pathways, which are initiated by NOS and IDO, respectively [12]. Nitric oxide inhibits IDO *in vitro*, and it is postulated that it regulates IDO activity *in vivo* [10]. Here we report the results of micro-synchrotron-radiation-induced x-ray emission (micro-SRIXE) experiments on the induction of IDO in mammalian cells (porcine aortic endothelial cells) with IFN γ and the effect on its induction by the presence of a NO source.

Methods and Materials

Whole cell samples of porcine aortic endothelial cells were prepared according to methods reported previously for photon-induced x-ray emission (PIXE) experiments on V79 Chinese hamster lung cells [16, 17]. The cells (approximately 10⁶) were treated with IFN γ in the presence or absence of a sodium nitroprusside, a source of NO. Following this, the cells were washed twice with phosphate-buffered saline (PBS) and harvested with 2% trypsin. The cell suspension was centrifuged, and the supernatant was replaced with PBS prior to final replacement with ammonium acetate solution (200 mM, Ajax). The cells were then mounted on 200 μ m London Finder grids coated with formvar, then freeze-dried.

Hard x-ray microprobe experiments were performed on SRI-CAT beamline 2-ID-D [18]. All measurements were conducted using a monochromatic 10-keV x-ray incident beam, and under a He atmosphere in order to eliminate the Ar K-shell fluorescence signal from air, which masked the Cl and K signals. A number of fluorescence maps were simultaneously collected for each two-dimensional scan. Each map corresponded to the integrated K α fluorescence signal of an element of interest. Elements analyzed were: P, Cl, K, Ca, Cr, Fe, Cu, and Zn.

Whole cells were analyzed using a beam that was focused to approximately 1- μm diameter using a phase-zone-plate-based scanning hard x-ray microprobe [19]. Individual cells on a gold transmission electron microscope (TEM) grid were located initially by collecting an x-ray transmission image of the sample with a charge-coupled device (CCD) camera placed behind a scintillator. This procedure enabled a single cell to be centered within a scan area that was generally $(20 \times 20) \mu\text{m}^2$. Scans were acquired in 1- μm steps and the emitted x-rays were detected for 3 s per point using a Canberra Ultra-LEGe germanium x-ray detector. The detector had an energy resolution of ~ 200 eV over the range of elements examined.

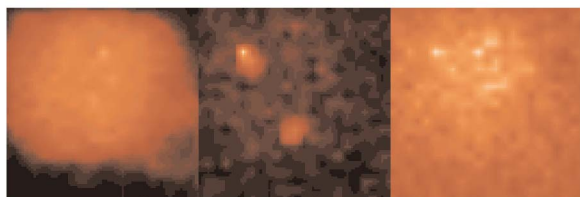
Signal integration was achieved during acquisition by software. An energy region for each fluorescence peak was defined before data collection and corresponded approximately to the area under the full width at half maximum of the peak.

Results

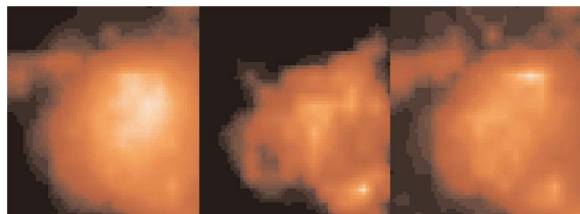
Fig. 1 shows P, Cr and Fe maps of a single control and IFN γ -treated porcine aortic endothelial cell. The P maps define the outline of the cells. For the control, there are hot spots of Cr, and Fe, although the Fe levels are only just above the background.

In the IFN γ -treated cells, there is a marked increase in the Fe content and all other elements to varying degrees, whereas in the presence of an NO source there is little change in the elemental distribution (Table 1). Micro-x-ray absorption near-edge structure (XANES) spectra of the Fe K edge (not shown) are typical of heme proteins [14, 20] and are different in the presence and absence of an NO source. The concentrations of both Cu and Zn increased 10-fold and 30-fold,

CONTROL CELL



IFN γ -TREATED CELL



P Cr Fe

FIG. 1. Elemental maps (arbitrary intensities) of a control and an IFN γ -treated cell.

Table 1. Elemental amounts (arbitrary units) within control and treated cells.^a

	Control	IFN γ	IFN γ + NO
P	0.003 \pm 0.0006	0.011 \pm 0.002	0.004 \pm 0.0006
S	0.004 \pm 0.0001	0.013 \pm 0.001	0.006 \pm 0.0009
Cl	0.026 \pm 0.00008	0.088 \pm 0.006	0.051 \pm 0.012
K	0.014 \pm 0.001	0.167 \pm 0.015	0.009 \pm 0.002
Ca	0.0021 \pm 0.0004	0.021 \pm 0.004	0.002 \pm 0.003
Cr	0.0003 \pm 0.00003	0.002 \pm 0.0005	0.0004 \pm 0.0001
Fe	0.0019 \pm 0.0004	0.011 \pm 0.003	0.0012 \pm 0.0005
Cu	0.003 \pm 0.0005	0.0296 \pm 0.005	0.028 \pm 0.003
Zn	0.005 \pm 0.0018	0.164 \pm 0.060	0.003 \pm 0.001

^a The errors are the standard deviations from 3-4 cells.

respectively, in IFN γ -treated cells and the Cu and Zn maps exhibited similar, (but not the same) intracellular distributions, whereas the intracellular distributions were distinctly different in the controls.

Discussion

Consistent with the anticipated effects of IFN γ on cells, there is a substantial increase in heme protein (presumed to be IDO) within the cells, whereas the concentration of the heme protein does not differ from normal levels in the presence of a NO source. It is not clear whether this is due to a regulatory role of NO [11], or whether the NO causes a general efflux of metal ions compared to treatment with IFN γ only.

The large increase in Cu and Zn in the intracellular maps on IFN γ treatment is likely to be due in part to the induction of superoxide dismutase because of the similarity in the maps. However, the greater increase in Zn and some differences in the localisation patterns in regions of high P content, may also be indicative of an increase in Zn finger proteins in response to the IFN γ .

The unusually high levels of Cr in both the control and treated cells may be a reflection of the use of Cr dietary supplements in pig feed.

Further research on both the induction of IDO and the presence of relatively high levels of Cr compared to other cells that have been analysed will be investigated in the future.

Acknowledgments

We are grateful for financial support from an Australian Research Council (ARC) Discovery Grant and a University of Sydney Sesqui Research and Development Grant (PAL), an ARC Australian Research Fellowship (PKW), and a National Health & Medical Research Council of Australia grant (RS). This research was supported by the Australian Synchrotron Research Program, which is funded by the Commonwealth of Australia under the Major National Research Facilities program. Use of the Advanced Photon Source was supported by the U.S. Department of Energy, Office of Science, Office of Basic Energy Sciences, under Contract No. W-31-109-ENG-38. We also acknowledge support from SRI-CAT.

References

- [1] O. Hayaishi, Biken J. **28**, 39-49 (1985).
- [2] Y. Sun, Mater. Med. Pol. **21**, 244-250 (1989).
- [3] M.W. Taylor, G. Feng, FASEB J. **5**, 2516-2522 (1991).
- [4] M. Sono, T. Taniguchi, Y. Watanabe, O. Hayaishi, J. Biol. Chem. **255**, 1339-1345 (1980).
- [5] M. Sono, J. Biol. Chem. **264**, 1616-1622 (1989).
- [6] M. Sono, J.H. Dawson, Biochim. Biophys. Acta **789**, 170-187 (1984).
- [7] M. Sono, Biochemistry **29**, 1451-1460 (1990).
- [8] F. Hirata, T. Ohnishi, O. Hayaishi, J. Biol. Chem. **252**, 4637-4642 (1977).
- [9] A.C. Terentis, S.R. Thomas, O. Takikawa, T.K. Littlejohn, R.J.W. Truscott, R.S. Armstrong, S.-R. Yeh, R. Stocker, J. Biol. Chem. **277**, 15788-15794 (2002).
- [10] S.R. Thomas, PhD Thesis, University of Sydney, Sydney (1998).
- [11] S.R. Thomas, P.K. Witting, R. Stocker, J. Biol. Chem. **271**, 32714-32721 (1996).
- [12] S.R. Thomas, D. Mohr, R. Stocker, J. Biol. Chem. **269**, 14457-14464 (1994).
- [13] L. Jia, C. Bonaventura, J. Bonaventura, J.S. Stamler, Nature **380**, 221-226 (1996).
- [14] A.M. Rich, R.S. Armstrong, P.J. Ellis, P.A. Lay, J. Am. Chem. Soc. **120**, 10827-10836 (1998).
- [15] D.V. Stynes, H.C. Stynes, B.R. James, J.A. Ibers, J. Am. Chem. Soc. **95**, 4087-4089 (1973).
- [16] C.T. Dillon, P.A. Lay, A.M. Bonin, M. Cholewa, G.J.F. Legge, T.J. Collins, K.L. Kostka Chem. Res. Toxicol. **11**, 119-129 (1998).
- [17] M. Cholewa, I.F. Turnbull, G.J.F. Legge, H. Weigold, S.M. Marcuccio, G. Holan, E. Tomlinson, P.J. Wright, C.T. Dillon, P.A. Lay, A.M. Bonin Nucl. Instrum. Methods B **104**, 317-323 (1995).
- [18] Z. Cai, B. Lai, W. Yun, P. Ilinski, D. Legnini, J. Maser, W. Rodrigues, Am. Inst. Phys. Proc. **507** (X-Ray Microscopy VI), 472-477 (2000).
- [19] W. Yun, B. Lai, Z. Cai, J. Maser, D. Legnini, E. Gluskin, Z. Chen, A.A. Krasnoperova, Y. Vladimirovsky, F. Cerrina, E. Di Fabrizio, M. Gentili, Rev. Sci. Instrum. **70**, 2238-2241 (1999).
- [20] A.M. Rich, R.S. Armstrong, P.J. Ellis, H.C. Freeman, P.A. Lay, Inorg. Chem. **37**, 5743-5753 (1998).